Z. angew. Math. Phys. 55 (2004) 1015–1033
0044-2275/04/061015-19
DOI 10.1007/s00033-004-2092-5

Zeitschrift für angewandte Mathematik und Physik ZAMP

Two-dimensional variational vibroequilibria and Faraday's drops

Ivan Gavrilyuk, Ivan Lukovsky and Alexander Timokha*

Abstract. When contacting with acoustically-vibrated structures a fluid volume can take a [time-averaged] geometric shape differing from capillary equilibrium. In accordance with theorems by Beyer *et al.* (2001) this shape (vibroequilibrium) furnishes a local minimum of a [quasi-potential energy] functional. The variational problem contains five dimensionless parameters evaluating the fluid volume, the wave number of acoustic field in the fluid domain, the contact angle and two newly-introduced numbers (η_1, η_2) giving relationships between (surface tension, gravitation) and Kapitsa's vibrational forces/energy. The paper focuses on negligible small wave numbers (incompressible fluid) and two-dimensional flows. Although the variational problem may in some isolated cases have analytical solutions, it requires in general numerical approaches. Numerical examples simulate experiments by Wolf (1969) and Ganiyev *et al.* (1977) on vibroequilibria in horizontally vibrating tanks. These show that there appear at least two types of stable vibroequilibria associated with symmetric (possible non-connected) and asymmetric surface shapes. The paper represents also numerical results on flattening and vibrostabilisation of a drop hanging beneath a vibrating plate (experiments by Faraday (1831)).

Mathematics Subject Classification (2000). 76N10, 35Q35.

Keywords. Vibroequilibria, minima principle, Nyström method, flattening drops.

1. Introduction

The problem on nonlinear interfacial sloshing of fluid-gas (two-fluid) systems in a tank performing translatory/rotational vibrations belongs to actual physical problems of wave hydrodynamics. The surveys by Nevolin (1984) [43], Lukovsky & Timokha (1999) [33], Perlin & Schultz (2000) [44], Faltinsen & Timokha (2001, 2002) [7, 8], Ibrahim *et al.* (2001) [16] and La Rocca *et al.* (2002) [25] include detailed description of theoretical and experimental results from this scientific field emphasising mainly nonlinear gravity/capillary-gravity waves due to resonant forcing. When forcing frequency is close to the lowest natural frequency, the resonant waves occur relative to potential equilibria caused by surface tension and gravitation. The potential equilibria coincide then with mean (time-averaged) fluid

*Corresponding author

shapes and play the role of a zero-order approximation in an appropriate asymptotic analysis (Faltinsen & Timokha (2002) [9]).

Requirements in new technologies for chemical industry and space material science motivate to develop acoustic (vibration) approaches for governing (positioning) either solid particles or fluid drops in a gaseous media. Experimental and theoretical results on the acoustic contactless positioning and exotic shapes of acoustically-levitated drops (acoustic equilibria) have been documented by Wang (1996) [47], Apfel *et al.* (1998) [2] and Lee *et al.* (1998) [29] (the Second United States Microgravity Lab), by Wanis *et al.* (1999) [48] (the NASA KS-135 space program) and by Lierke (1991) [30] (the MICREX experimental program of the European Space Agency).

A macroscopic fluid volume can also change its [time-averaged] shape due to contacts with acoustically-oscillated structures (vibroequilibria). This type of contact vibrational positioning goes back to Faraday (1831) [11]. Experimental series 39-52 of his manuscript describe the flattening of fluid drops hanging beneath a vibrating plate. The key experimental examinations of vibroequilibria have later been done by Wolf (1969, 1970) [49, 50], Lyubimov & Cherepanov (1981, 1986) [36, 35], Bezdenezhnikh *et al.* (1991) [5], Khenner *et al.* (1999) [23], Ivanova *et al.* (1997, 1998, 2001) [17, 18, 19, 20] and Lyubimov *et al.* (2002) [37]. Various kinds of vibrations and solid/elastic structures were tested. An emphasis was placed on interfacial vibroequilibria occurring in a horizontally vibrated tank: Wolf (1969) [49], Bezdenezhnikh *et al.* (1984) [4] and Ganiyev *et al.* (1977) [13] reported saw-tooth and inclined interfacial [time-averaged] reliefs for two-fluid and fluid-gas systems respectively. Theoretical analysis of the vibroequilibria was carried out by employing pendulum phenomenological models (Wolf (1969) [49]), numerical schemes and asymptotic technique (Lyubimov & Cherepanov (1986) [35] and Beyer *et al.* (2001) [3]). The asymptotic scheme uses vibroequilibria as zero-order approximation as well as associates their stability with dynamic stability of corresponding steady-state motions.

Both asymptotic analysis and computations for acoustic- and vibroequilibria were mainly related to relevant problems, where convectional flows are of principal concern (e.g., the influence of modulated gravity field on melt crystallisation studied by Anilkumar *et al.* (1993) [1] and Lee *et al.* (1996) [28]). There are however some physical situations when the fluid behaviour can be described in the framework of an inviscid fluid model with irrotational flows. These occur, for example, when the fluid density exceeds significantly the density of surrounding gas. Corresponding experimental results are given by Wolf (1969) [49], Ganiyev *et al.* (1977) [13] and Bezdenezhnikh *et al.* (1984) [4]. Assuming a perfect fluid with irrotational flows makes it possible to use the Lagrangian (Hamiltonian) variational technique adopted in resonant sloshing problems (Lukovsky & Timokha (1995) [32]). By accounting for this, Beyer *et al.* (2001) [3] have undertaken a mathematical activity aiming to derive a rigorous mathematical theory of vibroequilibria. By following the general concept of Vibrational Mechanics (Blekhman

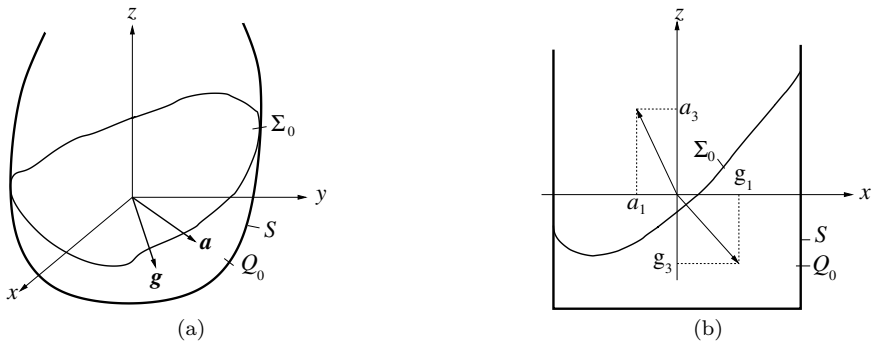

Figure 1. Sketch of a vibroequilibrium in the three-dimensional case (a), and in the framework of two-dimensional flows (b). The unit guiding vector $\mathbf{a} = (a_1, a_2, a_3)^T$, the frequency ν and the amplitude A are time independent constants. The fluid domain $Q_f(t)$ is confined to the wetted area $S_f(t) = \partial Q \cap \partial Q_f(t)$ and the free surface $\Sigma_f(t)$, so that $Q_0 = \langle Q_f \rangle$, $\Sigma_0 = \langle \Sigma_f \rangle$ and $S = \langle S_f \rangle$.

(1999) [6]) and results on the Lagrangian variational formalism for a compressible fluid (Lukovsky & Timokha (1995) [32]) they derived a quasi-potential energy functional. Local minima of this functional coincide with stable vibroequilibria. The functional collects terms associated with potential energy (surface tension and gravitation) as well as 'vibrational energy' based on the concept by Kapitsa (1952) [22]. The main advantage of the variational vibroequilibria is that it is symbolically equivalent to the problem on capillary meniscus. Notwithstanding, the original paper by Beyer *et al.* (2001) [3] gives neither qualitative nor numerical analysis of known vibro-phenomena. The present paper fills up this gap for incompressible and two-dimensional fluid flows in basins of rectangular shape.

2. Statement of the problem

Beyer *et al.* (2001) [3] have mathematically studied the free boundary problem on forced motions of a perfect compressible fluid $Q_f(t)$ (irrotational flows) in a rigid tank Q, which performs translatory harmonic high-frequency vibrations with velocity $\mathbf{v} = -\nu A \sin(\nu t)\mathbf{a}, ||\mathbf{a}|| = 1$. Following original assumptions of Vibrational Mechanics, Beyer *et al.* (2001) [3] considered small amplitude translatory vibrations (amplitude/tank size ratio $\epsilon = A/l \ll 1$) and the forcing frequency ν which exceeds significantly the primary natural frequency of the linear sloshing ν_0 (the last is caused by gravitation and surface tension), i.e. $\nu_0/\nu = O(\epsilon)$. They showed that the mean (time-averaged) free boundary $\Sigma_0 = \langle \Sigma_f \rangle$ is in this case governed by a free boundary problem which differs from the problem on capillary equilibria. The mean (time-averaged) domain $Q_0 = \langle Q_f \rangle$ bounded by $\Sigma_0 = \langle \Sigma_f \rangle$ and $S = \langle S_f \rangle$ became the name *"vibroequilibrium"* (see, Figure 1 (a)). Conclusions by Beyer *et al.* (2001) [3] are qualitatively consistent with known experimental results

and may methodologically be explained in terms of 'vibrational forces/energy' concept proposed by Kapitsa (1952) [22] and developed by Blekhman (1999) [6] for solid mechanical systems. Along with differential statement, the original paper by Beyer *et al.* (2001) [3] contains also the variational criterion of stability: *the vibroequilibrium Q_0 is dynamically stable, if and only if, it delivers a local minimum of the following functional*

$$\Pi_0(Q_0) = \eta_1(|\Sigma_0| - \cos\alpha|S|) - \eta_2 \int_{Q_0} (g_1 x + g_2 y + g_3 z) dQ + \\ + \int_{Q_0} (|\nabla\psi|^2 - k^2(\psi - a_1 x - a_2 y - a_3 z)^2) dQ \underset{Q_0}{\rightarrow} \min, \quad (2.1)$$

subjected to

$$Q_0 \subset Q; \quad \int_{Q_0} dQ = V = const \quad (2.2)$$

and

$$\Delta\psi + k^2\psi = k^2(a_1 x + a_2 y + a_3 z) \ in \ \ Q_0, \\ \partial_n\psi = 0 \ on \ \ S; \ \ \psi = a_1 x + a_2 y + a_3 z \ on \ \Sigma_0. \quad (2.3)$$

Here $|\cdot|$ is the area, ∂_n is the outer normal derivative to ∂Q_0, $\mathbf{g} = (g_1, g_2, g_3)$, $|\mathbf{g}| = 1$ is the unit guiding vector of gravitation, α is the contact angle, k is the wave number of acoustic field modulated in the fluid, V is the fluid volume.

Integral equation (2.2) defines the volume (mass) conservation rule. The Dirichlet-Neumann boundary value problem (2.3) expresses dependence of the [wave] function $\psi(x, y, z)$ on Q_0. The function ψ appears in the first-order approximation of steady-state fluid motions, namely, velocity potential of the original evolutional problem is posed in the form $\epsilon\psi(x, y, z)\cos(\nu t) + o(\epsilon)$ (mathematical details can be found in the original paper [3]). Physically, these high-frequency steady-state fluid motions are induced by vibrations of the tanks (rigid structure) and can only be possible due to mobility of $\Sigma_f(t)$ and compressible (acoustic) fluid flows (incompressible flows imply $k = 0$).

Beyer *et al.* (2001) [3] introduced two dimensionless numbers η_1 and η_2 calculated by formulae $\eta_1 = 4\mu$, $\eta_2 = -4\mu\mathrm{Bo}$, where $\mu = \sigma/(\nu^2 A^2 l\rho) > 0$, Bo=$gl^2\rho/\sigma$ ($\pm$Bo is the Bond number; the sign depends on direction of gravitation vector, see Myshkis *et al.* (1987) [40]), g is the gravity acceleration, ρ is the fluid density and σ is the coefficient of surface tension. Solutions of (2.1)-(2.2) (shapes Q_0) depend on five dimensionless parameters, i.e. V, α, k, η_1 and η_2. Further, the functional (2.1) can be considered as the sum of three physically different terms. First and second terms (at η_1 and η_2) express the contributions of surface tension and gravitation respectively. The ratio $|\eta_2/\eta_1| = |\mathrm{Bo}|$ is the gravitation/surface tension energy relationship (see, Myshkis *et al.* (1987, 1992) [40, 41] and Monti (2000) [39]). The third [integral] term of Π_0 implies so-called 'vibrational energy' (Blekhman (1999) [6]). 'Vibrational energy' amounts itself both the averaged (per forcing period) kinetic energy of steady-state fluid motions caused surface/interface waves and

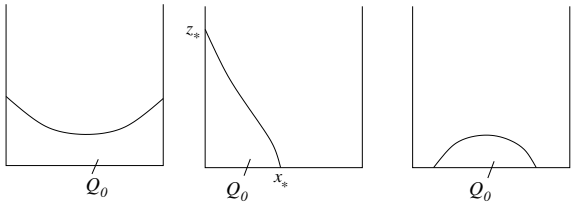

Figure 2. Three admissible vibroequilibria in a rectangular tank: (a) curvilinear trapezoid, (b) curvilinear triangle and (c) drop upon a plate (bottom).

the averaged (acoustic) energy associated with compressible fluid flows. Details on how these terms are derivable from the Lagrangian variational formulation of the original evolutional problem are given by Beyer *et al.* (2001) [3].

After assuming $k = 0$ (the incompressibility has early been postulated by Lyubimov *et al.* (1981) [36], Lyubimov & Cherepanov (1986) [35], Bezdenezhnikh *et al.* (1991) [5], in some exercises by Timokha (1992) [45], by Khenner *et al.* (1999) [23] and Ivanova *et al.* (2001) [19]) we will furthermore focus on vibroequilibria in a parallelepipedal tank Q with the vectors $\mathbf{g}$ and $\mathbf{a}$ to be coplanar to the Oxz-plane. When $k = 0$ the 'vibrational energy' (the last summand of Π_0) coincides with the averaged kinetic energy of steady-state wave fluid motions. Further, admissible domains Q_0 are single-connected with piece-smooth boundary shaped as shown in Figure 2. Let $2l$ be the tank breadth (the distance between walls parallel to the Oyz-plane) and $2L$ be the tank width (the distance between walls parallel to the Oxz-plane). Assumption $l/L \ll 1$ makes it under certain circumstances possible to neglect the meniscus along the Oy-axis and reduces the original problem (2.1)–(2.3) to the following formulation in the Oxz-plane

$$\Pi(Q_0) = \eta_1(|\Sigma_0| - \cos\alpha|S|) - \eta_2 \int_{Q_0} (g_1 x + g_3 z) dQ + \int_{Q_0} |\nabla\psi|^2 dQ \underset{Q_0}{\to} \min, \quad (2.4)$$

subjected to the following two-dimensional boundary value problem

$$\Delta\psi = 0 \ \text{ in } \ Q_0; \quad \partial_n\psi = 0 \ \text{ on } \quad S; \quad \psi = a_1 x + a_3 z = w(x,z) \ \text{ on } \ \Sigma_0 \qquad (2.5)$$

and the volume conservation condition (2.2). Here, in accordance with denoting in Figure 1 (b), Q_0, S and Σ_0 deal with their traces on the Oxz-plane, such that $|\cdot|$ is the length of corresponding curves.

3. Method

3.1. Analytical solution

Faraday (1831) [11], Wolf (1969, 1970) [49, 50] and Bezdenezhnikh *et al.* (1984) [4] have experimentally shown that high-frequency vertical vibrations ($\mathbf{a}||\mathbf{g}$) of

the tank can dynamically stabilise the Rayleigh–Taylor interfacial instability of the planar potential equilibrium. The review by Nevolin (1984) [43] treats this point as vibration-induced stability by parametric excitation of a multidimensional nonlinear system. One way to obtain corresponding theoretical conclusions is to involve the Mathieu analysis of small free surface perturbations. The use of the variational formulation (2.4), (2.5), (2.2) is an alternative approach.

When capillary meniscus has planar shape perpendicular to $\mathbf{g} = (0, 0, g_3)^T$, $g_3 = 1$ (gravity acceleration is directed upward) and $\alpha = \pi/2$, it becomes unstable due to the Rayleigh-Taylor instability for (Myshkis *et al.* (1987, 1992) [40, 41])

$$-\mathrm{Bo} = \frac{\eta_2}{\eta_1} > \varkappa_1^2, \quad \varkappa_1 = \frac{\pi}{2}. \tag{3.6}$$

Assuming $\mathbf{a}||\mathbf{g}$ makes it possible to find the analytical solution of (2.4), (2.5), (2.2). It is $z = 0$ (horizontal planar vibroequilibrium) and $\psi =$const. By employing the positiveness of the Jacobi operator of (2.4) or, alternatively, the positiveness of its spectrum (explicit form of the Jacobi operator was derived by Beyer *et al.* (2001) [3]) we arrive at the criterion of stability for the planar vibroequilibrium as follows

$$\eta_2 < \eta_1 \varkappa_1^2 + \varkappa_1 \tanh(\varkappa_1 h). \tag{3.7}$$

Comparing (3.6) and (3.7) deduces that even if (3.6) holds true (unstable capillary surface), (3.7) can be fulfilled (the vibroequilibrium is stable) for sufficiently small $\eta_1 = O(1/\nu^2)$ and $\eta_2 = O(1/\nu^2)$ due to the passage $\nu \to \infty$.

Another analytical solution

$$\psi = C_1 = \mathrm{const}; \quad a_1 x + a_3 z = C_1, \tag{3.8}$$

of (2.4), (2.5), (2.2) exists for $\eta_1 = \eta_2 = 0$ ($\nu = \infty$). Here Π holds its absolute minimum ($\Pi = 0$) and Σ_0 is as shown in Figures 3 (a-c).

Experiments by Wolf (1969, 1970) [49, 50] and Bezdenezhnikh *et al.* (1984) [4] described also vibrational phenomena, which cannot easily be related to vibration-induced parametric stabilisation. This is for instance an 'inclined' stationary interfacial relief occurring in horizontally-vibrated tank ($\mathbf{a} \perp \mathbf{g}$) along the Ox-axis. Wolf (1969) [49] and Timokha (1997) [46] have intuitively explained this inclination by using a pendulum phenomenological model of sloshing (see details on pendulum modelling in sloshing problems by Ibrahim *et al.* (2001) [16]). The analysis of the pendulum dynamics due to high-frequency external forcing is for instance given by Kapitsa (1952) [22], Landau & Lifschitz (1962) [26] and Blekhman (1999) [6].

3.2. Numerical method

Vibroequilibria should in general case be found from a numerical minimisation of (2.4) subjected to (2.5) and (2.2). The algorithm must consist in selecting an admissible class of Q_0 with its appropriate parametrisation/discretisation $Q_0 =$

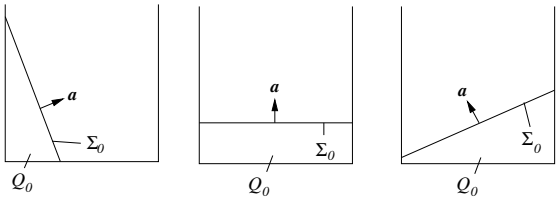

Figure 3. Sketch of possible stable vibroequilibria for extremely large forcing frequency $\nu = \infty$ ($\eta_1 = \eta_2 = 0$). The planar free boundary Σ_0 is perpendicular to the guiding vector $\mathbf{a}$.

$Q_0(d_1, \ldots, d_{M1})$, $d_i \in \mathbb{R}$ and in matching a robust numerical scheme for the Dirichlet-Neumann boundary value problem (2.5). The solver of (2.5) must keep uniform accuracy for any admissible $Q_0(d_1, \ldots, d_{M_1})$.

Furthermore, we assume for domains in Figure 2 that Σ_0 allows either $z = f(x)$ or $x = f(z)$ normal form equation. The function $f(\cdot)$ will in numerical schemes be associated with a cubic spline by Forsythe *et al.* (1977) [12]

$$f(\cdot) \cong A_i(f_k) + B_i(f_k)(\cdot\ -\ \cdot_i) + C_i(f_k)(\cdot\ -\ \cdot_i)^2\ + D_i(f_k)(\cdot\ -\ \cdot_i)^3, \qquad (3.9)$$

where A_i, B_i, C_i, D_i are functions of $f_k = f(\cdot_k)$ defined in the mesh points $\cdot_k$, $k = 0, \ldots, M$, $M \geq 4$. Since this spline technique does not need any additional conditions at endpoints of the interval $[\cdot_0, \cdot_M]$, Q_0 becomes a function of $\{f_k, k = 0, \ldots, M\}$. The variables $\{f_k\}$ are subjected to volume conservation condition (2.2). In order to avoid this restriction we will use a re-parametrisation $f_k = f_k(d_i), k = 0, \ldots, M$ aiming to satisfy (2.2) for the independent variables $\{d_k \in \mathbb{R},\ k = 0, \ldots, M1\}$. Proceeding this way, the functional Π becomes a function of $\{d_k, k = 1, \ldots, M1\}$.

The minimisation needs both solution $\psi \in W_2^1(Q_0)$ of (2.5) and computation of the last integral term in (2.4). Using Green's formula for this integral term

$$\int_{Q_0} (\nabla\psi)^2 dQ = \int_{\Sigma_0} \partial_n\psi\ w\ d\Gamma$$

implies that its calculation needs only the Neumann trace $\partial_n\psi$ on Σ_0. Hence, the boundary element methods for (2.5) seem to be a most efficient approach to our variational problem.

Let $P(\xi, \eta) \in \partial Q_0$ and $P^*(x.z) \in Q_0$ be two arbitrary points on the boundary and in open part of Q_0 respectively. When using representation of a harmonic function via single and double layer potentials we get (Mikhlin (1977) [42] p. 207)

$$\psi(x, z) = \frac{1}{2\pi} \oint\limits_{\partial Q_0} \left[\ln \frac{1}{R} \partial_{n_P}\psi - \psi \partial_{n_P} \ln \frac{1}{R} \right] d\Gamma_P, \qquad (3.10)$$

where $R = R(\xi, \eta; x, z) = \sqrt{(\xi - x)^2 + (\eta - z)^2}$. Here $\ln \frac{1}{R}$ is the two-dimensional free space Green function and $\mathbf{n}_P$ means a unit vector normal from ∂Q_0 in the

point P pointing out of the domain Q_0. In accordance with the rules for single and double layer potentials the integral representation (3.10) can be traced on the boundary and re-written as follows

$$\omega_{(x,z)}\psi(x,z) = \oint\limits_{\partial Q_0} \left[\ln\frac{1}{R}\partial_{n_P}\psi - \psi\partial_{n_P}\ln\frac{1}{R}\right] d\Gamma_{(\xi,\eta)}, \tag{3.11}$$

where $P^*(x,z) \in \partial Q_0$ and $\omega_{(x,z)}$ is the solid angle at $P^*(x,z)$ ($\omega_{(x,z)} = \pi$ for smooth pieces of the boundary).

The Dirichlet trace $\psi = w(x,z)$ is known on Σ_0, while the Neumann trace $\partial_n\psi = 0$ is given on the remaining part S. Then for $P^* \in \partial Q_0$ the integral representation (3.11) yields the integral equation on ∂Q_0 as follows

$$\begin{aligned}\int_{\Sigma_0}\left[\Phi\ln\frac{1}{R} - w\partial_{n_{(\xi,\eta)}}\ln\frac{1}{R}\right]d\Gamma_{(\xi,\eta)} - \int_S \Psi\partial_{n_{(\xi,\eta)}}\ln\frac{1}{R}d\Gamma_{(\xi,\eta)} = \\ = \omega_{(x,z)}\begin{cases} w(x,z), & (x,z)\in\Sigma_0; \\ \Psi(x,z), & (x,z)\in S,\end{cases}\end{aligned} \tag{3.12}$$

where $\partial_{n_P} = \partial_{n_{(\xi,\eta)}}$. This integral equation couples two unknown functions

$$\Phi = \partial_n\psi \ \text{ on } \ \Sigma_0; \quad \Psi = \psi \ \text{ on } \ S \tag{3.13}$$

and falls, in fact, into a system of integral equations defined on smooth pieces of ∂Q_0. ∂Q_0 in Figure 2 consists at most of four smooth portions. The most complex case (curvilinear trapezoid) is presented in Figure 2 (a). The integral equation (3.12) takes in this case the following form

$$\begin{aligned}&\int_{-1}^{1}\Phi(\xi)\sqrt{1+f'^2(\xi)}\left[\ln\frac{1}{R}\right]_{\eta=f(\xi)}d\xi - \\ &-\int_{-1}^{1}w(\xi)\left[\partial_\eta\ln\frac{1}{R} - f'(\xi)\partial_\xi\ln\frac{1}{R}\right]_{\eta=f(\xi)}d\xi + \int_0^{f(-1)}\Psi_-(\eta)\left[\partial_\xi\ln\frac{1}{R}\right]_{\xi=-1}d\eta - \\ &-\int_0^{f(1)}\Psi_+(\eta)\left[\partial_\xi\ln\frac{1}{R}\right]_{\xi=1}d\eta + \int_{-1}^{1}\Psi_0(\xi)\left[\partial_\eta\ln\frac{1}{R}\right]_{\eta=0}d\xi = \\ &= \pi\begin{cases} w(x,f(x)), & z=f(x), \ -1<x<1; \\ \Psi_0(x), & z=0, \ -1<x<1; \\ \Psi_-(z), & x=-1, \ 0<z<f(-1); \\ \Psi_+(z), & x=1, \ 0<z<f(1),\end{cases}\end{aligned} \tag{3.14}$$

where the Neumann trace $\Phi = \Phi(x) \in W^{-1/2}[-1,1]$ was previously defined in (3.13) and the Dirichlet trace Ψ is a continuous function on flat portions S_- (wetted left wall), S_+ (wetted right wall) and S_0 (bottom). When taking into account the regularity results by Grisvard (1985) [15], Ψ falls into three functions

(densities)

$$\Psi = \begin{cases} \Psi_0(x), & -1 < x < 1; \\ \Psi_-(z), & 0 < z < f(-1); \\ \Psi_+(z), & 0 < z < f(1); \end{cases} \quad \Psi_0(-1) = \Psi_-(0); \quad \Psi_0(1) = \Psi_+(0). \quad (3.15)$$

The system of integral equations (3.14) couples the unknowns Φ, Ψ_0, Ψ_- and Ψ_+. The integral kernels of (3.14) are explicitly calculated by Gavrilyuk & Timokha (2003) [14] for admissible domains in Figures 2 (a,b). Several those kernels are of regular character (or have removable singularities) in closed domains of definition. Other kernels have either logarithmic singularity (associated with single layer potential terms) or power singularity (associated with the double layer potential) at the corner points (endpoints). Solution ψ and, therefore, the unknown densities Φ, Ψ_0, Ψ_+ and Ψ_- have almost always the singularities at the corner points (Lukovsky *et al.* (1984) [31] and Grisvard (1985) [15]). Singular character of double layer potential kernels and densities depends dramatically on both the contact angle and the curvature of Σ_0. This means that boundary element schemes may have significant error and need a refining mesh procedure even with slightly varying Q_0. This may cause time-inefficient computations.

We analysed appropriate boundary element algorithms based on integral systems alike (3.14). Typical papers can be exemplified by Misuno & Kodama (1990) [38] and Landrini *et al.* (1999) [27] implementing boundary element scheme for time-stepping in the evolutional fluid sloshing problem. As matter of fact, Misuno & Kodama (1990) [38] ignored the corner singularities, while Landrini *et al.* (1999) [27] only discussed them. Since these papers consider nearly-rectangular domains Q_0 with nearly-right contact angle between Σ_0 and S (in terms of our definitions), the solution ψ is of singular character only for higher derivatives. However, duly various geometrical variations of Q_0 the solution ψ may have the corner singularities in the first derivatives. Their capturing becomes therefore of primary concern. An example of an appropriate boundary element scheme taking into account the corner singularities is given by Kress (1990) [24]. He develops it for the Dirichlet boundary value problem. Since this Kress-Nyström scheme produces appropriate mesh grading automatically (depending on Q_0), it does not need a refining mesh procedure with changing Q_0. Authors have modified this scheme for the Dirichlet-Neumann problems (Gavrilyuk & Timokha (2003) [14]). Details and convergence theorems will be presented in a forthcoming publication.

4. Numerical results and discussion

Numerical results below have been obtained with maximum dimensions $M = 20$ (the number of mesh points for spline approximation of Σ_0) and $N_1 = ... = N_4 = 50$ (the number of mesh points on smooth portions of ∂Q_0). Numerical procedure required typically $N_1 \approx ... \approx N_4 \approx 30$ and $M = 10$ to get 4-5 steady digits for an uniform approximation of Σ_0. The maximum dimensions were used to calculate

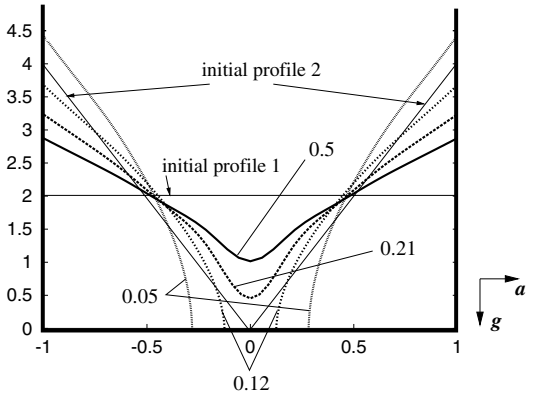

Figure 4. The Oz-symmetric two-dimensional vibroequilibria for $\eta_1 = 0$ (earth-based conditions) and $V = 4$ ($h = 2$). The vibroequilibria are labelled by values of η_2. 'Initial profile 1' is used to calculate single-connected solutions ($\eta_2 = 0.5$ and 0.21). Disconnected domains are calculated with 'initial profile 2' ($\eta_2 = 0.12$ and 0.05). The critical value of η_2, for which vibrations separate the fluid into two equal subdomains, is predicted about 0.205.

'critical' vibroequilibria, at which Q_0 undergoes separation into two sub-volumes. The procedure of numerical minimisation adopted a quasi-Newton method by Kahaner *et al.* (1988) [21]. The iteration number depended on number of mesh points and was typically between 5 and 50. Calculations have been done on a Pentium-II-366 computer. Calculation time has been affected by $\eta_1,\ \eta_2, M, N_1, \ldots, N_4$ and initial approximation of Σ_0. It was typically (for our non-optimised FORTRAN-code) between 15-600[s].

4.1. Vibroequilibria in a horizontally vibrating tank

Wolf (1969) [49], Ganiyev *et al.* (1977) [13] and Bezdenezhnikh *et al.* (1984) [4] established experimentally two typical vibroequilibria occurring in a horizontally vibrating tank filled by a fluid-gas system ('gas density'/'fluid density'$\ll 1$). The first one consists in an 'inclination' (re-orientation) of the fluid. Σ_0 becomes geometrically close to an inclined plane. These vibroequilibria belong to the Oz-asymmetric admissible shapes in Figure 2 (b). The second type of vibroequilibria deals with the Oz-symmetric solutions, such that Σ_0 forms a 'cavity'-like profile (Ganiyev *et al.* (1977) [13] published corresponding photos). The fluid volume may in the last case be separated by horizontal vibrations into two equal sub-volumes localised at opposite walls.

Vibroequilibria under terrestrial conditions ($\eta_1 = 0$). A macroscopic fluid volume under terrestrial conditions is characterised by large Bond numbers (Myshkis *et al.* (1987, 1992) [40, 41] and Monti (2000) [39]). This implies $|1/\mathrm{Bo}|=|\eta_1/\eta_2| \ll$

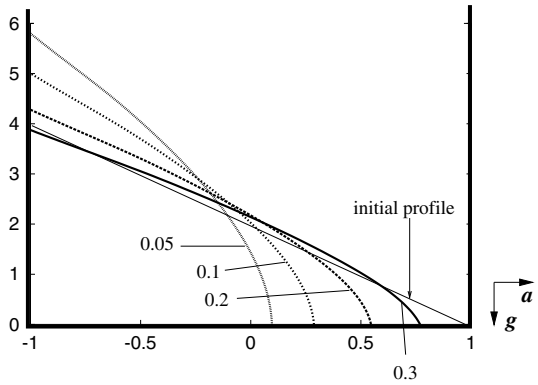

Figure 5. Asymmetric vibroequilibria under terrestrial conditions ($\eta_1 = 0$) for $V = 4$ obtained with triangular 'initial profile' as an initial approximation of Σ_0. The vibroequilibria are labelled by values of η_2. Stable asymmetric vibroequilibria do not exist for $\eta_2 > 0.302$.

1. Assuming $|\eta_2| = O(1)$ gives $|\eta_1| \ll 1$. This means that surface tension is negligible relative to gravitation and 'vibrational energy'. We will therefore adopt $\eta_1 = 0$. In turn, α disappears from the functional Π. Solutions of the variational problem (2.4), (2.5), (2.2) become then depending on two parameters η_2 and V (dimensionless mean fluid depth $h = V/2$). We centre numerical simulations around the case $h = O(1)$. Shallow and intermediate fluid depth (Lukovsky & Timokha (2000) [34] and Faltinsen & Timokha (2002) [8] estimated them for $h \lesssim 0.24$) as well as fairly deep fluid depths are not analysed. Depending on initial approximation of Σ_0, η_2 and h the computations give either symmetric or asymmetric profiles Σ_0. There are also the pairs (η_2, h), for which these solutions co-exist. This means that the problem (2.4), (2.2), (2.5) may be not uniquely solvable (it has, at least, two local minima).

A typical strategy to distinguish co-existing solutions (vibroequilibria) consists in performing the numerical minimisation with different initial boundary shapes. Each such an initial shape can physically be treated as an instantaneous wave pattern occurring in transients when vibrational forcing starts. We used two transient scenarios characterised by different wave patterns. The first scenario suggests easily that there are no transients (transient waves of negligible small amplitude). The second one suggests asymmetric, triangular profile (see, Figure 5) associated with instantaneous wave profiles (bores, run-up etc.) of large amplitude mentioned and illustrated by Faltinsen & Timokha (2002) [8]. Some numerical results, presented in Figures 4 and 5, exemplify how these two scenarios lead to different vibroequilibria.

The vibroequilibria with $\eta_2 = 0.5$ and 0.21 in Figures 4 were obtained by assuming the first transient scenario. The computations used the horizontal 'initial profile 1'. Whenever $\eta_2 > 0.205$, this initial position of Σ_0 in our iterative min-

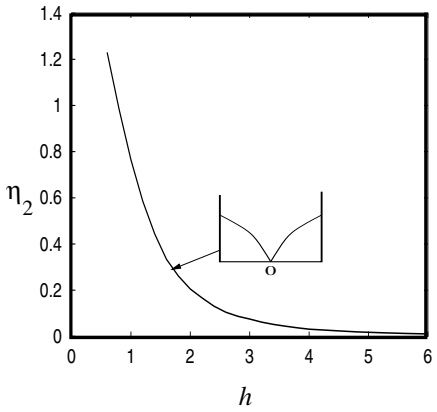

Figure 6. The critical pairs (h, η_2) at which the symmetric single-connected vibroequilibria become disconnected ones. Earth-based conditions ($\eta_1 = 0$).

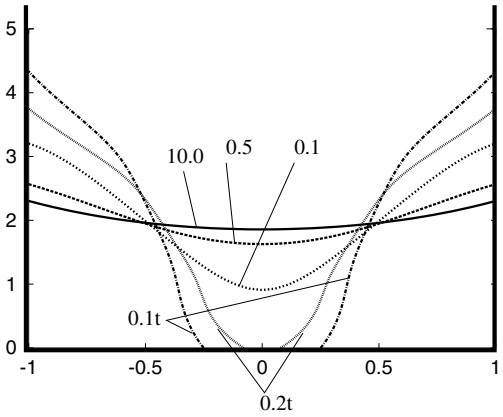

Figure 7. The Oz-symmetric two-dimensional vibroequilibria for $\eta_2 = 0$ (zero-gravitation conditions), $\alpha = \pi/4$ and $V = 4$. The vibroequilibria are labelled by values of η_1. 'Initial profile 1' (see Figure 4) was used to calculate single-connected solutions ($\eta_1 = 10.0, 0.5$ and 0.1) 'Initial profile 2' in Figure 4 was adopted to calculate non-connected vibroequilibria labelled by $0.2t$ and $0.1t$ (for $\eta_1 = 0.2$ and 0.1 respectively).

imisation procedure leads to axial-symmetric Q_0. For $\eta_2 \leq 0.205$ the numerical scheme can diverge due to intersection between Σ_0 and the bottom. The second transient scenario assumed triangular initial approximations of Q_0 ('initial profile' in Figure 5). Whenever $\eta_2 < 0.302$, this initial approximation in the iterative procedure leads to asymmetric Σ_0. Some examples are presented in Figure 5. These asymmetric solutions are absent for $\eta_2 > 0.302$ due to their instability.

Hence, for $\eta_1 = 0, V = 4$ and $\eta_2 > 0.302$ our two initial transient scenarios give

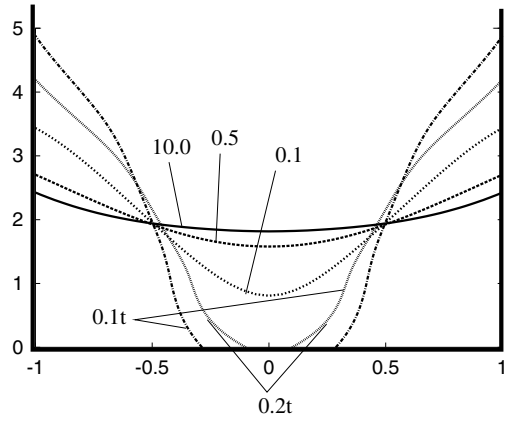

Figure 8. The same as in Figure 7, but $\alpha = \pi/6$.

exclusively symmetric stable vibroequilibria, but when $0.205 < \eta_2 < 0.302$ both symmetric and asymmetric vibroequilibria are found. Asymmetric vibroequilibria exist also for $\eta_2 < 0.205$ (see examples in Figure 5). For $\eta_2 < 0.205$ the fluid can also fall into two equal Oz-symmetric portions. The developed algorithm makes it possible to find these vibroequilibria with 'initial profile 2' shown in Figure 4 (see examples with $\eta_2 = 0.12$ and 0.05 in Figure 4).

It is of especial interest to find critical pairs (η_2, h), at which the fluid separates Oz-symmetrically into two sub-volumes. This point for each such a sub-volume deals with condition $x_* = 0$ depicted in Figure 2 (b). By using this condition for each sub-volume we found the dependence η_2 versus h and presented it in Figure 6. The graph demonstrates, that critical η_2 increases with decreasing h and, therefore, smaller fluid volumes are separated by vibrational with lower excitation frequency (because $\eta_2 = O(1/\nu^2)$). The splitting (separation) would hardly occur for fairly deep fluid, because critical $\eta_2 \to 0$ as $h \to \infty$, and, therefore, critical $\nu \to \infty$.

Vibroequilibria under zero-gravity conditions ($\eta_2 = 0$). For zero-gravity (microgravity) conditions $|\mathrm{Bo}| = |\eta_2/\eta_1| \ll 1$ (Myshkis *et al.* (1987, 1992) [40, 41] and Monti (2000) [39]). Solutions of (2.4), (2.5), (2.2) depend then on three dimensionless numbers V, η_1 (we assume $\eta_1 = O(1)$ and, in turn, $\eta_2 = 0$) and α. When following two transient scenarios introduced above (starting minimisation from either planar or triangular initial profiles), the computations demonstrate both symmetric and asymmetric solutions. These appear in the same way as it was described in the previous paragraph. There are only minor local geometric differences at the contact points influenced by the different contact angles. Corresponding numerical examples are given in Figures 7 and 8. We should note that our previous calculation strategy to estimate critical pairs (h, η_1), at which the fluid may split into two symmetric portions, fails. This is due to a hysteresis in

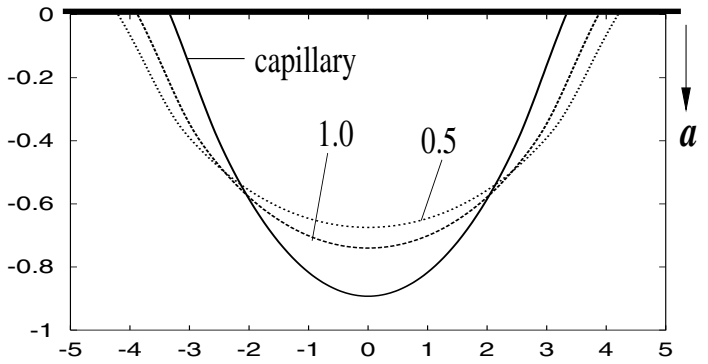

Figure 9. Flattening capillary drop with decreasing $\eta_1 = O(1/\nu^2)$ (increasing forcing frequency ν) on a vibrating plate. Zero-gravity conditions ($\eta_2 = 0$), $V = 2$ and $\alpha = \pi/6$. The curves are labelled by η_1.

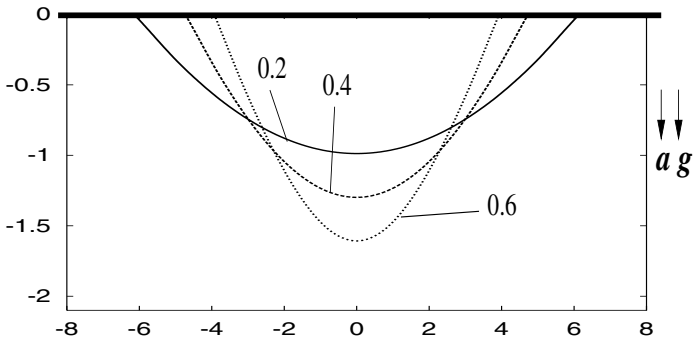

Figure 10. Stabilisation and flattening of a drop hanging beneath a vibrating plate. $\eta_1 = 0$, $V = 4$. The curves are labelled by the values of η_2. Critical value of η_2, when the drop becomes unstable due to Rayleigh-Taylor instability is estimated near $\eta_2 = 0.73$.

the dependence between η_1 and h. Significant region of η_1 is found, where both single-connected and disconnected symmetric solutions co-exist. Corresponding profiles in Figures 7 and 8 are exemplified by 0.1 and 0.1t. These profiles were obtained with the same $\eta_2 = 0, V = 4, \alpha = \pi/4$ ($\pi/6$) and $\eta_1 = 0.1$, but for different initial approximations (transient scenarios). The hysteresis can be explained by a jump of the surface energy (due to the surface tension) established in different capillary problems (Myshkis *et al.* (1987) [40]).

4.2. Vibroequilibria of a drop on a vibrating plate

The capillary equilibria of a drop on a rigid plate were in details investigated by Myshkis *et al.* (1987, 1992) [40, 41]. When these drops are modified by vertical vibrations (Faraday (1831) [11]) both the variational vibroequilibria concept and the proposed numerical technique can be used. Flattening drop with decreasing η_1 (increasing ν) is exemplified in Figure 9. The calculations are consistent with Faraday's experimental observations.

Vibrations of the plate may significantly influence the drop extent occurring with increasing Bond number (η_2) and prevent its fall from the plate (the drop becomes unstable for non-small Bond numbers due to the Rayleigh-Taylor instability). Our test computations emphasise the limit case $\eta_1 = 0$ and $\eta_2 = O(1)$ (this means infinite Bond number, i.e. $|\eta_2/\eta_1| = |\mathrm{Bo}| \gg \infty$). When there are no vibrations, conditions $\mathrm{Bo} \gg 1$ and $g_3 = -1$ (gravitation is directed downward) lead immediately to fall of the drop from the plate (Myshkis *et al.* (1987) [40]). In contrast, the numerical solutions in Figure 10 demonstrate stable vibroequilibria. The critical η_2, at which the drop becomes unstabile and falls from the vibrating plate is found near 0.73.

5. Conclusions

Two-dimensional vibroequilibria of a limited incompressible fluid volume are examined. These may occur in a parallelepipedal tank forced harmonically with high frequency. Further, the gravity acceleration and guiding vibration vectors are coplanar and belong to the Oxz-plane. The analysis is based on variational concept by Beyer *et al.* (2001) [3]. The variational formulation contains the terms associated with surface tension, gravitation and Kapitsa's vibrational energy.

1. When surface tension and gravitation are negligible small relative to Kapitsa's vibrational energy ($\eta_1 = \eta_2 = 0$) we found an analytical solution of the variational problem delivering an absolute minimum of the corresponding functional. The time-averaged free surface is then perpendicular to the direction of vibration.
2. For vertical vibrations the variational concept explains analytically the vibration-induced stability by parametric excitation (stabilisation of the Rayleigh-Taylor instability), which was for instance described experimentally by Wolf (1970) [50].
3. The governing functional is subjected to the Dirichlet-Neumann boundary problem. We approximate its solution by a modified boundary element method by Kress (1990) [24], which handles the singularity at the corner points. The method provides an automatic mesh grading. The actual vibroequilibria under terrestrial (large Bond number) and microgravity conditions (small Bond number) in a horizontally vibrating rectangular container are numerically studied. It is shown that vibration may both separate the fluid domain into two equal sub-domains (splitting) and ensure the fluid volume near one of vertical walls (inclination, re-

orientation). The vibroequilibria depend on the dimensionless numbers η_1 and η_2, the mean fluid volume and initial approximation of the free surface. The dependence of the vibroequilibria on its initial approximation in iterative procedure can be treated as the influence of different transient wave patterns (transient scenarios) occurring when the vibroforcing starts and means non-uniqueness of solution. The experimental observations by Wolf (1969) [49], Bezdenezhnikh *et al.* (1984) [4] and Ganiyev *et al.* (1977) [13] are qualitatively described.

4. Vibrostabilisation and the flattening of a drop hanging beneath a vibrating plate are described (Faraday (1831) [11]). It was shown that the Rayleigh-Taylor instability can be stabilised by vibrations even if the surface tension is neglegibly small (large Bond numbers).

5. Even if $k = 0$ (incompressible fluid) and the problem is considered in two-dimensional statement there are two serious numerical difficulties to find the vibroequilibria. The first one gives rise from analytical description of admissible vibroequilibria, on which the functional should be minimised, and their discretisation. In particular, the domain can be separated into two and more subdomains due to vibroloading (homogenization). The second difficulty consists in matching the minimisation with solving the Dirichlet-Neumann boundary value problem constraining the test vibroequilibrium and the wave function. Some additional efforts are required to overcome these difficulties for the three-dimensional case and $k \neq 0$ (compressible flows). The additional problem for the three-dimensional case is a significantly wider set of possible initial transients scenarios (see Faltinsen, Rognebakke & Timokha (2003) [10] discussing some three-dimensional nonlinear wave patterns occurring for transients).

Acknowledgement

A. T. is grateful for financial support made by the Alexander-von-Humboldt Foundation. Other authors acknowledge partial support made by the German Research Council (DFG).

References

[1] A. V. Anilkumar, R. N. Grugel, X. F. Shen and T. G. Wang, Control of thermocapillary convection in a liquid bridge by vibration, *J. Appl. Phys.* **73** (1993), 4165–4170.

[2] R.E. Apfel, Y. Tian, J. Jankovsky, T. Shi, X. Chen, R.G. Holt, E. Trinh, A. Croonguist, K.C. Thornton, A.Jr. Sacco, C. Colemen, F.W. Leslie and D.H. Matthiesen, Free oscillations and surfactant studies of superdeformed drops in microgravity, *Phys. Rev. Let.* **78** (1998), 1912–1915.

[3] K. Beyer, I. Gawrilyuk, M. Günther, I. Lukovsky and A. Timokha, Compressible potential flows with free boundary. Part I: Vibrocapillary equilibria, *ZAMM* **81** (2001), 261–271.

[4] N. K. Bezdenezhnikh, B. A. Briskman, D. V. Lyubimov, A. A. Cherepanov and M. T. Sharov, Control of stability of two-fluid interface by means of vibrations, electric and magnetic fields.

In Abstracts of the all-Union Seminar on Hydromechanics and Heat- and Mass Transfer, Chernogolovka 1984, 18-20 (Russian).

[5] N. A. Bezdenezhnikh, V. A. Briskman, A. Yu. Lapin, D. V. Lyubimov, T. P. Lyubimova, A. A. Tscherepanov and I. V. Zakharov, The influence of high-frequency tangential vibrations on stability of the fluid interface in microgravity. *In Proceedings of IUTAM Symposium "Microgravity Fluid Mechanics", Bremen 1991* Springer, Berlin 1992, 137–144.

[6] I. I. Blekhman, *Vibrational Mechanics.* World Scientific, Singapore 1999

[7] O. M. Faltinsen and A. N. Timokha, Adaptive multimodal approach to nonlinear sloshing in a rectangular tank, *J. Fluid Mech.* **432** (2001), 167–20.

[8] O. M. Faltinsen and A. N. Timokha, Asymptotic modal approximation of nonlinear resonant sloshing in a rectangular tank with small fluid depth, *J. Fluid Mech.* **470** (2002), 319–357.

[9] O. M. Faltinsen and A. N. Timokha, Analytically-oriented approaches to two-dimensional fluid sloshing in a rectangular tank (survey), *Proceedings of the Institute of Mathematics of the NASU* **44** (2002), 321–345.

[10] O. M. Faltinsen, O. F. Rognebakke and A. N. Timokha, Resonant three-dimensional nonlinear sloshing in a square base basin, *J. Fluid Mech.* **487** (2003), 1–42.

[11] M. Faraday, On a peculiar class of acoustic figures and on certain forms assumed by groups of particles upon vibrating elastic surfaces, *Phil. Trans. Roy. Soc. Lond.* **121** (1831), 299–430.

[12] G. E. Forsythe, N. A. Malcolm and C. B. Moler, *Computer Methods for Mathematical Computation.* Prentice-Hall, New York 1977.

[13] R. F. Ganiyev, V. D. Lakiza and A. S. Tsapenko, On dynamic behaviour of a free liquid surface under low gravity and vibrational effects, *Prikladnaya Mekhanika (Soviet Applied Mechanics)* **13** (1977), 102–107 (Russian).

[14] I. Gavrilyuk and A.Timokha, A Nyström-Kress scheme for a Dirichlet-Neumann boundary value problem associated with fluid sloshing in a rectangular tank, *Proceedings of the Institute of Mathematics of the NASU* **47** (2003), 284–301.

[15] P. Grisvard, *Elliptic Problems in Nonsmooth Domains.* Pitman, Boston 1985.

[16] R. A. Ibrahim, V. N. Pilipchuk and T. Ikeda, Recent advances in liquid sloshing dynamics, *Appl. Mech. Rev.* **54** (2001), 133–199.

[17] A. A. Ivanova, V. G. Kozlov and J. C. Legros, Mean dynamics of two liquid system in a cavity subjected to rotational vibrations. *In Proc. Joint 10th Europ. and 6th Russian Symp. Phys. Sci. in Microgravity, St.Petersburg, Russia 1997* Intst. Probl. Mech. RAS, Moscow **1** (1997), 280–283.

[18] A. A. Ivanova, V. G. Kozlov, D. V. Lyubomov, T. P. Lyubimova, S. Merady and B. Roux, Structure of averaged flow driven by a vibrating body with a large-curvature edge, *Fluid Dyn.* **33** (1998), 656–665.

[19] A. A. Ivanova, B. G. Kozlov and P. Evoux, Interfacial dynamics of two-liquid system under horizontal vibrations, *Izvestiya RAN. Mekhanika Zhidkosti i Gasa (Fluid Dynamics)* N 3 (2001), 28–35 (Russian).

[20] A. A. Ivanova, V. G. Kozlov and S. I. Tasjkinov, Interfacial dynamics of two-liquid system due to rotational vibrations (experiments), *Izvestiya RAN. Mekhanika Zhidkosti i Gasa (Fluid Dynamics)* N 6 (2001), 114–121 (Russian).

[21] D. Kahaner, C. Moler and S. Nash, *Numerical Methods and Software.* Prentice-Hall, New York 1988.

[22] P. L. Kapitsa, The pendulum with a vibrating point of suspension, *Adv. Phy. Sc.* **44** (1952), 34–42 (Russian).

[23] M. V. Khenner, D. V. Lyubimov, T. S. Belozerova and B. Roux, Stability of plane-parallel vibrational flow in a two-layer system, *Eur. J. Mech. B/Fluids* **18** (1999), 1085–1101.

[24] R. Kress, A Nyström method for boundary integral equations in domains with corners, *Numer. Math.* **58** (1990), 145–161.

[25] M. La Rocca, G. Sciortino and M. Boniforti, Interfacial gravity waves in a two-fluid system, *Fluid Dyn. Res.* **30** (2002), 31–66.

[26] L. D. Landau and E. M. Lifschitz, *Mechanik.* Akademie-Verlag, Berlin 1962.
[27] M. Landrini, G. Grytøyr and O.M. Faltinsen, A B-spline based BEM for unsteady free-surface flows, *J. Ship Res.* **43** (1999), 13–24.
[28] C. P. Lee, A. V. Anilkumar and T. G. Wang, Streaming generated in a liquid bridge due to nonlinear oscillations driven by the vibrations of an endwall, *Phys. Fluids* **8** (1996), 3234–3246.
[29] C. P. Lee, A. V. Anilkumar, A. B. Hmelo and T. G. Wang, Equilibrium of liquid drops under effects of rotation and acoustic flattening: Results from USML-2 experiments in space, *J. Fluid Mech.* **354** (1998), 43–67.
[30] E. G. Lierke (*eds.*), Acoustic positioning. *In Summary Review of Sounding Rocket Experiments in Fluid Science and Material Sciences (post-flight); TEXUS 1 to 20, MASTER 1 and 2*, ESA SP-1132, February 1991, 362-365.
[31] I. A. Lukovsky, M. Ya. Barnyak and A. N. Komarenko, *Approximate Methods of Solving the Problems of the Dynamics of a Limited Liquid Volume.* Naukova dumka, Kiev 1984 (Russian).
[32] I. A. Lukovsky and A. N. Timokha, *Variational Methods in Nonlinear Dynamics of a Limited Liquid Volume.* Institute of Mathematics, Kiev 1995 (Russian).
[33] I. A. Lukovsky and A. N. Timokha, Nonlinear theory of sloshing in mobile tanks: classical and non-classical problems (survey). *In book "Problems of analytical mechanics and its applications"*, Institute of Mathematics of NASU, Kiev 1999, 169–200 (Russian).
[34] I. A. Lukovsky and A. N. Timokha, Steady-state nonlinear sloshing in a rectangular tank: passage to shallow water, *Reports of National Academy of Sciences of Ukraine* (2000), 48–51.
[35] V. D. Lyubimov and A. A. Cherepanov, Development of a steady relief at the interface of fluids in a vibrational field, *Fluid Dyn.* **21** (1986), 849–854.
[36] D. V. Lyubimov, A. A. Cherepanov and V. A. Briskman, Control of the fluid free surface by fluctating fields. *In Abstracts of II All-Union Seminar on Hydromechanics and Heat- and Mass Transfer, Perm 1981*, Perm 1981, 112–114 (Russian).
[37] D. V. Lyubimov, T. P. Lyubimova, R. V. Skuridin, G. Chen and B. Roux, Numerical investigation of meniscus deformation and flow in an isothermal liquid bridge subject to high-frequency vibrations under zero gravity conditions, *Computers & Fluids* **31** (2002), 663–682.
[38] Akisato Mizuno and Yoshihiro Akisato, Analysis of nonlinear wave–making phenomena by means of boundary element method, *Res. Repts. Kogakuin Univ.* **69** (1990), 15–20 (Japanese).
[39] R. Monti (*ed.*), *Fluid Physics in Microgravity.* Reading Overseas Publishing Associates 2000.
[40] A. D. Myshkis, V. G. Babsky, N. D. Kopachevskii, L. D. Slobozhanin and A. D. Typsov, *Low-Gravity Fluid Mechanics. Mathematical Theory of Capillary Phenomena.* Springer-Verlag, Berlin Heidelberg 1987.
[41] A. D. Myshkis, V. G. Babsky, M. Yu. Zhukov, N. D. Kopachevskii, L. D. Slobozhanin and A. D. Typsov, *Methods for Solving Hydromechanic Problems in Zero-Gravity.* Naukova dumka, Kiev 1992 (Russian).
[42] S. G. Mikhlin, *Linear Partial Differential Equations.* Vishaya shkola, Moscow 1977 (Russian).
[43] V. G. Nevolin, Parametric excitation of surface waves (survey), *Inzhenerno-Physicheskiy Zhurnal* **47** (1984), 1028–1042 (Russian).
[44] M. Perlin and W. W. Schultz, Capillary effects on surface waves, *Annu. Rev. Fluid Mech.* **32** (2000), 241–274.
[45] A. N. Timokha, Behaviour of the free surface of a fluid in a vibrating bounded vessel. *Preprint N 22, Akad. Nauk Ukrainy Inst. Mat.* Institute of Mathematics, Kiev 1992 (Russian).
[46] A. N. Timokha, Effect of lateral vibration of a tank on free surface of the fluid, *Technical Mechanics* **5** (1997), 33–41 (Russian).
[47] T. Wang, Drop physics module / drop dynamics experiment. *In 90-day Science Report of the Second United States Microgravity Laboratory (USML-2), March 1996*, 69–71.

[48] S. Wanis, A. Sercovich and N. Komerath, Acoustic shaping in microgravity: higher order surface shapes, *AIAA Paper N 99-0954* (1999).
[49] G. H. Wolf, The dynamic stabilisation of the Rayleigh-Taylor instability and the corresponding dynamic equilibrium, *Z. Physik* **227** (1969), 291–300.
[50] G. H. Wolf, Dynamic stabilisation of the interchange instability of a liquid-gas interface, *Phys. Rev. Lett.* **24** (1970), 444–446.

Ivan Gavrilyuk
Berufsakademie Thüringen-Staatliche Studienakademie
D-99817 Eisenach
Germany

Ivan Lukovsky
Institute of Mathematics
National Academy of Sciences of Ukraine
01601 Kiev
Ukraine

Alexander Timokha
Institute for Applied Mathematics
Friedrich-Schiller-Universität Jena
D-07743 Jena
Germany

(Received: October 17, 2002; revised: June 30, 2003)